



Direct Measurements of Turbulence and Flow Characteristics of a Vertical Axis Wind Turbine Using the Eddy Covariance Method

Y. M. H'ng, Y. Yusup*

Environmental Technology, School of Industrial Technology, Universiti Sains Malaysia, USM 11800, Pulau Pinang, Malaysia.

PAPER INFO

Paper history:

Received 3 August 2015

Accepted in revised form 23 December 2015

Keywords:

EC method

Turbulence

Vertical axis wind turbine

ABSTRACT

Turbulence intensity measurements of vertical axis wind turbine (VAWT) are essential to determine its efficiency and performance. In this study, the eddy covariance (EC) method was used to characterise the flow and directly measure turbulence of a VAWT in a controlled indoor laboratory using an ultrasonic anemometer (at 10 Hz) at specific grid positions of upwind and downwind (in the wake) of the VAWT. In contrast to numerical simulations, this method has the potential to accurately quantify turbulence of wind turbines and thus able to describe the flow patterns around a VAWT experimentally. Results show that at the upwind position, some of the swept area of the VAWT obstructed the flow due to the counter current flow generated by the VAWT rotors' rotation while causing some flows to be diverted and concentrated to the concurrent flow area of the VAWT. In the wake of the VAWT, flow velocities and turbulence decreased and dispersed while at the centre line, vertical turbulence decreased towards the bottom (ground) swept area. This downward transfer of turbulence caused generally negative vertical momentum transfer. However, a slight increase of turbulence was observed at the ground surface due to flow deflection.

doi:10.5829/idosi.ijee.2016.07.02.01

INTRODUCTION

Due to increasing global interest in finding sustainable energy resources, wind energy has been determined to be one "green" energy option that has great potential to contribute to the world's energy demands of the future [1]. Generally, there are two types of wind turbines: the horizontal axis wind turbine (HAWT) and the vertical axis wind turbine (VAWT), both capable to convert kinetic energy of the wind to electrical energy. HAWTs is more efficient in harvesting wind energy than VAWTs, but VAWTs perform better than HAWT in turbulent flow conditions [2]. Thus, the VAWT is deemed to be more suited to urban areas where turbulence is high and that the VAWT can be installed on buildings rooftops to access higher wind speed conditions [3, 4] while providing "direct-to-user" electrical energy to the VAWT-installed building.

Turbulence is created due to the unsteady flow and fluctuations of the three flow velocity components and can be quantified from its instantaneous deviation from

the mean flow velocity. Turbulent flow consists of different sizes of "eddies". Eddy is defined as the swirling unit of air in the turbulent flow. In this study, flow velocity is measured in three dimensions using the eddy covariance (EC) method. The EC method is widely used in quantification of the turbulent fluxes in the micrometeorology field and has also been implemented in a pilot study on the turbulence flow of a VAWT [5]. Using this method, flow velocities are separated into the longitudinal, lateral and vertical velocities components, analogous to the Cartesian x , y , and z axes, and are commonly denoted as u , v and w .

Research has found that by arranging VAWTs close to each other, the array of VAWTs could harvest more wind energy through vertical transfer of kinetic energy of turbulence or eddies [6, 7]. In this context, we focused on an individual VAWT instead of an array of VAWTs. Although there are numerous studies on numerical simulations of wind turbine flows [8-13], there are limited literature on direct measurements of flow and turbulence characteristics of VAWTs. Breton et al. [14]

*Corresponding author: Yusri Yusup
E-mail: yusriy@usm.my
Tel: +604-653-5201; Fax: +604-653-6375

revealed that the upstream distance between turbines affect turbine performance and hence the turbulence distribution pattern in front of a turbine was observed and presented in this work in addition to the wake (or downwind) of the VAWT. Numerical modeling tends to underestimate turbulence and flow fields [15], and thus, by using the EC method, this paper presents a comprehensive direct measurements of turbulence and flow of upwind and wake of the VAWT.

MATERIALS AND METHODS

Laboratory setup

This study was conducted in an indoor research laboratory to avoid the complex and uncontrollable flow fields outdoors because of the interaction between wind turbines and the atmospheric boundary layer, the atmospheric boundary layer is the atmospheric layer closest to the surface of the Earth. Rooftop monitoring of VAWT conducted by Tabrizi et al. [16] and reviews of factors affecting performance of a Savonius wind turbine [13] have provided some useful information towards this study. Furthermore, the latter layer is not commonly “neutral” where the effects of buoyancy could alter the flow fields under “unstable” conditions. Neutral is defined as when mechanical shear dominates buoyancy effects on turbulence production.

Three-dimensional side view of the laboratory layout is shown in Figure 1. Three units of 26" industrial standing fans with fan blades length of 0.35 m, were used to generate the flow field and were arranged in a row as shown in Figure 2a. To study the turbulence and flow characteristics of a 300 W Darrieus-type VAWT (iWind Energy, iW301, Taiwan), with total swept area of 1.44 m², an ultrasonic anemometer (81000, Young, USA) was used to measure the three-flow velocity components (u , v , w). The data was logged to a personal computer using a RS232 cable and HyperTerminal software (Microsoft, USA) as the interface. Sampling frequency of 10 Hz was averaged for 60-min (averaging time). From preliminary analysis, it was discovered that even 5-min averaging period was sufficient to capture all turbulence-scale fluxes, typically of 1-s period.

This experiment was conducted at two speed settings (“low” and “high” speeds) at four different configurations. The averaged mean flow velocity at low speed setting was approximately 3.2 m s⁻¹ while at high speed setting was 4.0 m s⁻¹ with Reynolds number of 1.31×10^8 (low speed setting) and 1.63×10^8 (high speed setting). At low speed setting, VAWT rotates within the range of 75–79 RPM (rotation per minute); while at at high speed setting, VAWT was at 101–105 three flow velocity components, u , v and w at 10 Hz. Data was collected for 60 min and processed using MATLAB (ver.

2012A, MathWorks, USA) using a custom data processing script. The processing algorithm includes quality control steps, such as spikes removal caused by electronic-signal noises, stationary tests, and Haar transform (used to identify the discontinuities in the time series data during the data quality check).

The mean flow velocity, \bar{u} , and the standard deviations of the fluctuations of the three flow velocities, such as velocities from the mean were calculated and denoted as σ_u , σ_v , and σ_w or turbulence. The three flow velocity fluctuations were calculated according to Eqs. (1), (2) and (3), whereby the mean lateral and vertical flow velocities, \bar{v} and \bar{w} were approximately zero. This method is known as the Reynolds decomposition method of flow velocities to separate the turbulent components from the mean flow velocity components.

$$u = \bar{u} + u' \quad (1)$$

$$v = \bar{v} + v' \quad (2)$$

$$w = \bar{w} + w' \quad (3)$$

RESULTS AND DISCUSSION

VAWT mean flow velocity and turbulence distribution patterns

Heat map was used to visualised the flow and turbulence distribution patterns of four different positions of the ultrasonic anemometer and VAWT, where each “cells” represents the measurement

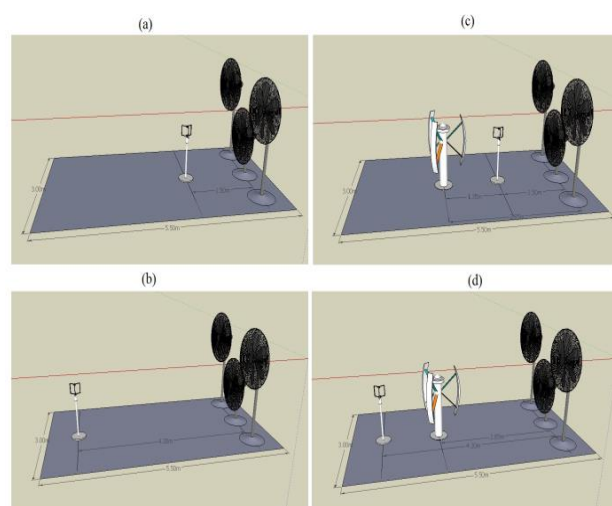


Figure 1. Laboratory setup depicting the arrangement of the ultrasonic anemometer, VAWT and the three 26" industrial standing fans at four different positions: a) upwind without VAWT; b) downwind without VAWT; c) upwind with VAWT; d) downwind with VAWT.

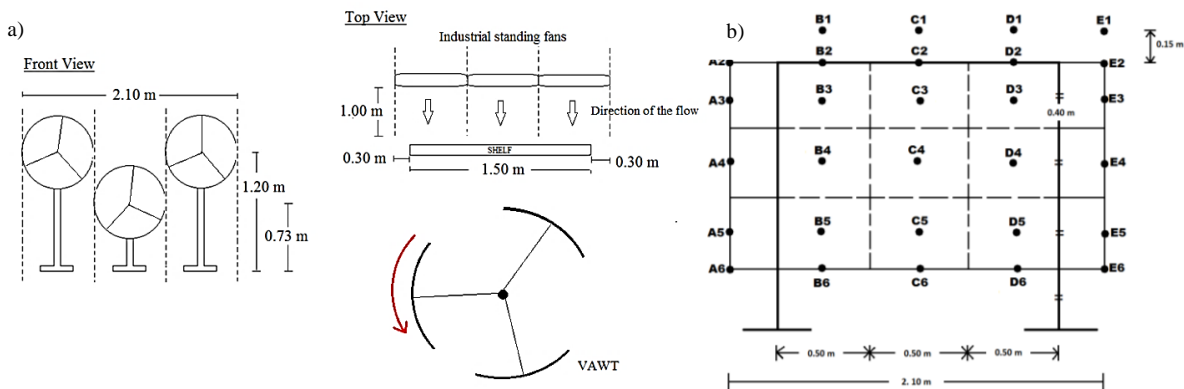


Figure 2. a) The front and top view of the arrangement of the three 26" industrial standing fans and b) fabricated shelf grid with 30 data collection positions (A1 to E6) covering the entire swept area of the flow source, which represents the flow field.

positions marked by the grid shelf. The turbulence patterns of upwind and wake of the VAWT flow fields were studied laterally and vertically. Results showed that the distribution for low speed and high speed were the same albeit at lower magnitudes for the low speed. This is because the design of the VAWT (which was constant) is the major factor in developing the flow field and thus the turbulence distribution irrespective of flow velocities. Furthermore, the pattern changed only when the VAWT was within the flow, which means that the downwind with VAWT flow and turbulence distribution patterns originated from the VAWT and not from the flow source (i.e., the fans). Thus, the results and discussion presented onwards refers only to the high speed flow field. The distributions of the mean flow velocity and turbulence for high speed setting at four different positions are shown in Figure 3, which displayed a classic turbulence energy cascade pattern for the downwind with VAWT runs.

Time series of mean flow velocities (averaged 5-min blocks) for a duration of 60 min, for upwind and downwind positions with and without VAWT within the flow is shown in Figure 4. As the trend of the time series of all positions were somewhat similar, only one position (E6) was selected to represent the time series trends. At upwind positions with or without VAWT (see Figure 4 a and c), the cycle of the incoming flow occurred every 10 to 15 min. However, the pattern of the 5-min block mean flow velocities at downwind positions occurred at a lower frequency of more or equal to 60 min (refer Figure 4 b and d). This reveals the frequency-scale difference between the incoming flow at upwind and downwind positions and indicates the generation of different flow patterns between the upwind (the fans) and downwind flows (the VAWT) as exhibited in Figure 3. Figures 3a and 3c show that the mean flow velocity distribution patterns are proximate at both upwind positions (with and without VAWT). Flow dispersed from upwind to

downwind, causing the flow velocities at downwind positions to reduce, refer to Figure 3b. With the VAWT placed at the downwind position, mean flow velocity behind the entire swept area of the VAWT was lower than without VAWT, refer to Figure 3d. In the middle column (column C) of the wind swept area behind the VAWT, mean flow velocity decreased when approaching the bottom surface. The mean flow velocity above the centre was higher due to the higher energy flow of this row layer [7].

Generally, the VAWT disperses the flow downwind; flow field transferred downwind partitioned into three distinct flow fields (or vortices) [17]. The highest flow velocity was observed in column E shown in Figure 3d due to the concurrent rotational direction (anti-clockwise) of the VAWT. Mean flow velocity were directed and concentrated in column E (the right-most column) by the VAWT where the flow is least obstructed due to the concurrent direction of the rotors. In column E, the mean flow velocity magnitude was two to three times higher compared with other columns while the mean flow velocity increased and decreased from top to bottom. The second highest mean flow velocity was observed in column A, but with the rotors moving counter current to the direction of the flow. Thus, flow velocities was directed to the concurrent column of the VAWT, The highest resistance, taken as highest occurrence of turbulence before the VAWT, of flow occurs in column D, C, and B (in order of magnitude) due to a small degree of reverse flow especially in cells D2, C3 and B3. Figure 5 illustrates the reverse flow generated by VAWT, showing the distribution of the flow due to the rotational direction of the VAWT. The blocking effect of turbine on the incoming flow from upwind has contributed to the slight decrease of mean flow velocity in column C and this is aligned with the observation found in Kinzel's work [7].

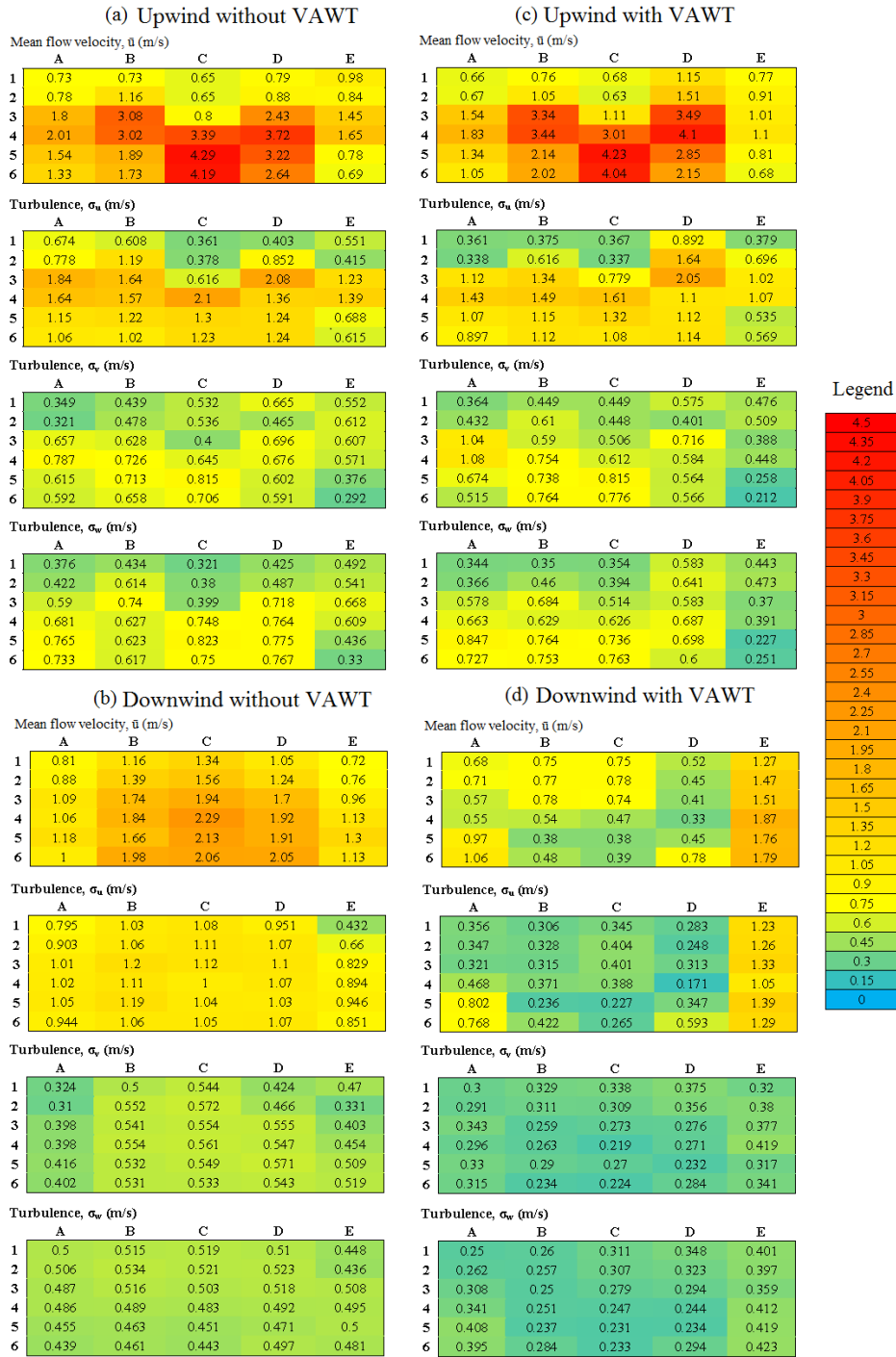


Figure 3. Along or longitudinal view of mean flow velocity, \bar{u} , and turbulence intensities, $\sigma_{u,v,w}$ distribution for the entire swept area covered by the flow source of three 26" industrial standing fans at high speed for four positions; (a) upwind position without VAWT; (b) downwind position without VAWT; (c) upwind position with VAWT; (d) downwind position with VAWT; each cell represents mean values measured for each position of the shelf grid (A1 to E6), columns A through E and rows 1 to 6.

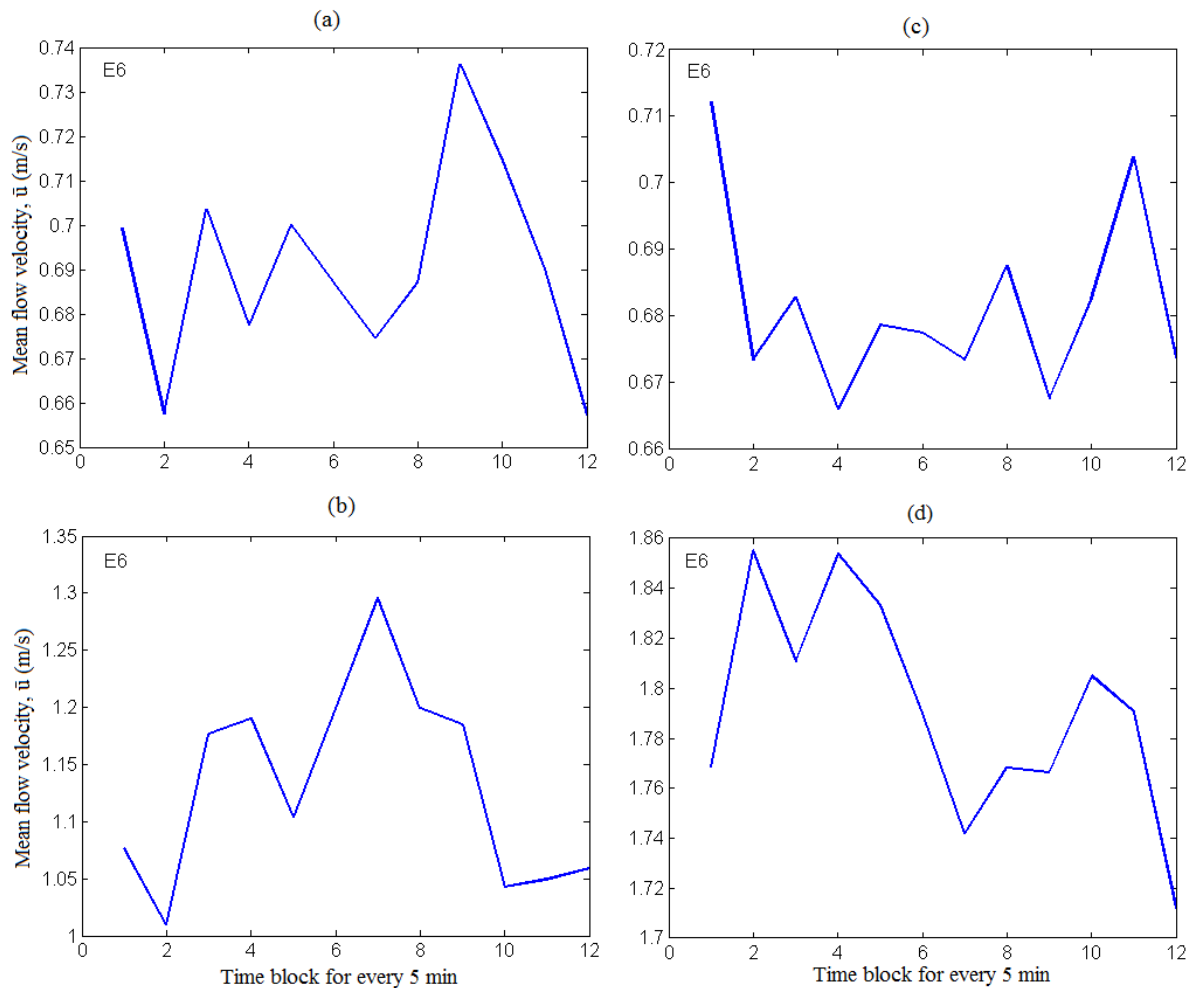


Figure 4. Time series of mean flow velocities, \bar{u} for four positions; (a) upwind position without VAWT; (b) downwind position without VAWT; (c) upwind position with VAWT; (d) downwind position with VAWT.

Lateral and vertical profile of VAWT turbulence

The turbulence (σ_u , σ_v , and σ_w) for upwind and downwind were also studied laterally and vertically. For upwind conditions with a VAWT, a build-up of turbulences σ_v and σ_w occurred in the general left wind swept area of the VAWT, columns A to D and rows 2 to 6 that suggest a diversion/blocking of flows.

Regardless of the VAWT, upwind turbulence was relatively the same possibly due to similar sources (i.e., the fans). The mean flow velocity and σ_u distribution were high, mainly due to the positioning of the flow source only at a distance of 1.5 m away from the ultrasonic anemometer (refer to Figures 3a) while the highest σ_u was located at the centre cell (C4) possibly due to the blocking effect of the VAWT mast. With the VAWT within the flow and at the upwind position, the lateral turbulence, σ_v , decreased linearly from cell A4 to cell E4 (Figure 3a). The trends for σ_w

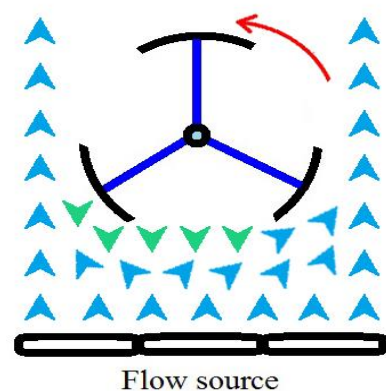


Figure 5. A sketch of the top view of the VAWT; flow directions of the VAWT rotor is represented by blue arrows; reverse flow generated by VAWT is represented by green arrows; the red thin arrow shows the rotational direction of the rotor; flow source is from the bottom.

were the same for both with and without VAWT within the flow. A slight decrease at cell E4 could be due to the effects of obstructions at the perimeter of the layout.

Turbulence dispersion took place downwind, whereby σ_u , σ_v and σ_w generally decreased without the VAWT. Placing the VAWT within the flow at the downwind position further decreased turbulence due to generally low mean flow velocities. Referring to Figure 3c, there were more turbulence and restrictions to flow in the bottom right column. Comparing the lateral profile of the downwind positions with and without VAWT, Figure 6 shows that σ_u was higher in column E when VAWT is within the flow except for E1, which was located at the top row covered by the swept area. The counter-clockwise rotation of the VAWT contributed in the increase of mean flow velocity in column E. The VAWT created vortices with vortex shedding, which caused the turbulence intensity to increase in column E.

A higher value of σ_u at column E is observed due to the concurrent rotational direction of the VAWT, as mentioned earlier. The lateral profiles of σ_v and σ_w are shown in Figure 7. From row 3 to row 6, σ_v and σ_w were lower in areas within column B to D compared with the edge of the covered swept area, which were columns A and E. This was also reported in numerical simulation, which showed a bell-shaped velocity deficit that occurred behind a HAWT [17]. Here, we also observed that turbulence (lateral and vertical) were at its highest in the middle position and downwind of the swept area of VAWT.

The efficiency of a VAWT not only depends on its longitudinal mechanical energy-extraction capability but also on its ability to extract vertical momentum flux energy. Comparing the vertical mean flow velocity and σ_u distributions at upwind positions, both situations were mainly dependent on the positioning of the measurement location. Due to the flow being dispersed downwind by the VAWT, the mean flow velocity reduced as shown previously. A vertical profile of σ_u shows the effect of VAWT on turbulence in its wake as shown in Figure 8.

Wind speed was approximately zero at the bottom wind swept area and so momentum has transferred downwards into the surface. At the downwind position without VAWT, flow dissipated towards the bottom or surface, σ_u decreased and eddies sizes nearer to the ground become small. With the VAWT within the flow and at the downwind position, σ_u and σ_v reduced. The remaining turbulence, which dissipated downwind was extracted by the VAWT. There is a slight increase in σ_u and σ_v at the bottom wind swept area, indicated by red colour circles in Figure 8. At this bottom area near the edge of the VAWT, kinetic energy was reflected back into the flow by the surface. This could be caused by the flows that contacted the surface of the ground, which generated secondary vortices due to the blocking effect and caused the slight increase of σ_u behind the VAWT [18]. Vertical momentum transfers from top to bottom when VAWT was within the flow. Referring to Figure 9, in the area behind the VAWT and at column C, σ_w decreased. The σ_w reduced vertically from top to bottom at a higher rate compared to σ_u and σ_v .

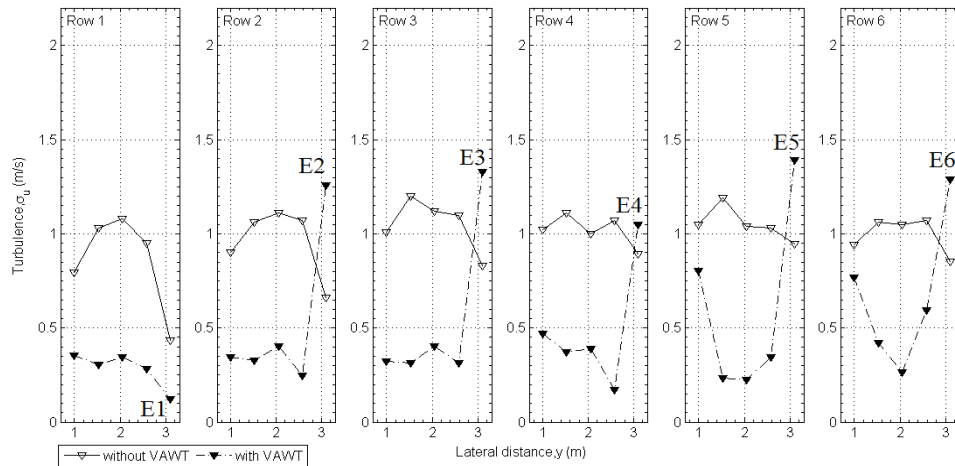
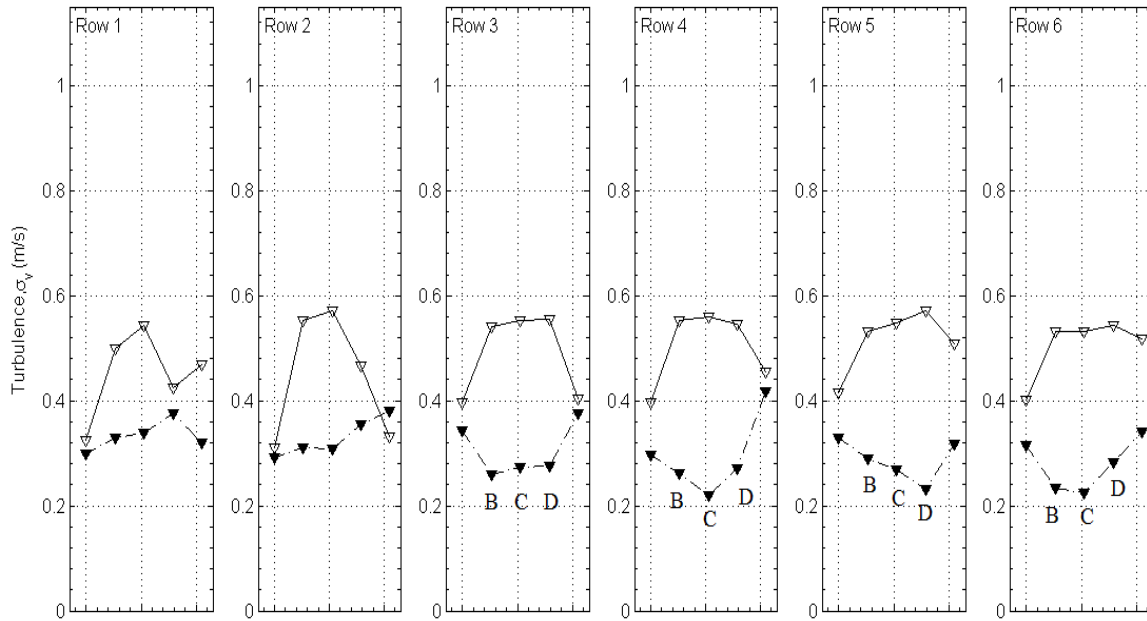


Figure 6. Lateral profile of longitudinal turbulence intensity, σ_u , from the left column to the right column (A to E) for each row (1 to 6) at high speed at downwind position; inverted triangle symbol represents downwind position without VAWT while filled inverted triangle symbol represents downwind position with VAWT.

(a) σ_v



(b) σ_w

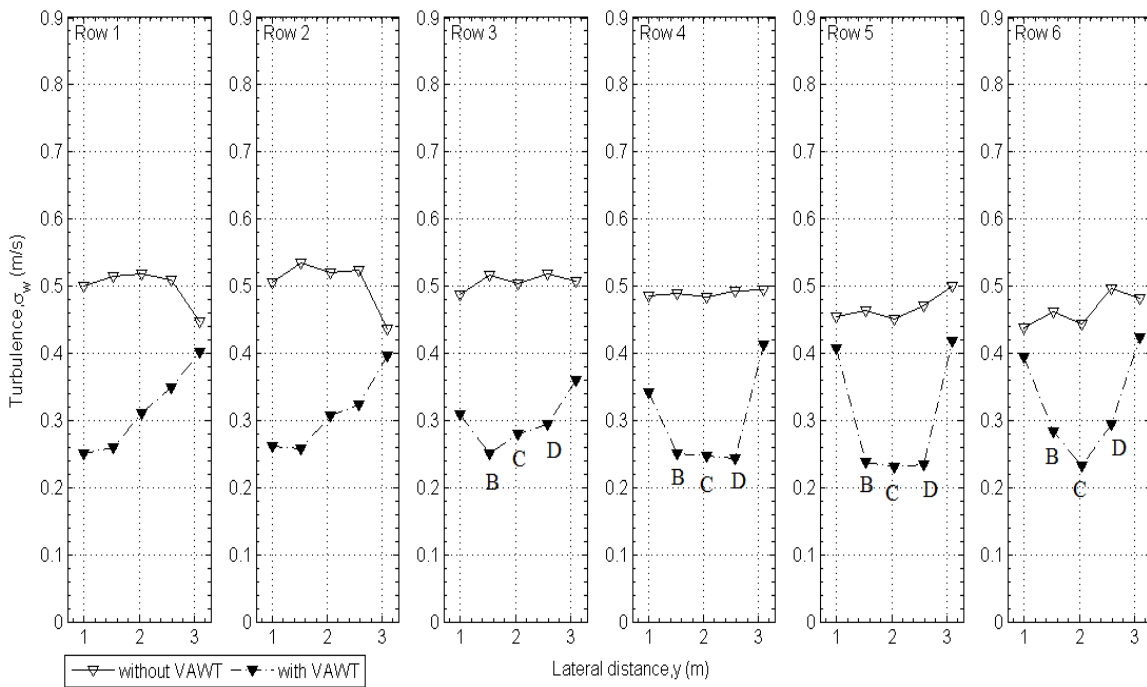


Figure 7. Lateral profile of lateral and vertical turbulence intensities (σ_v and σ_w) distribution from the left column to the right column (A to E) for each row (1 to 6) at high speed at downwind position; inverted triangle symbol represents downwind position without VAWT while filled inverted triangle symbol represents downwind position with VAWT

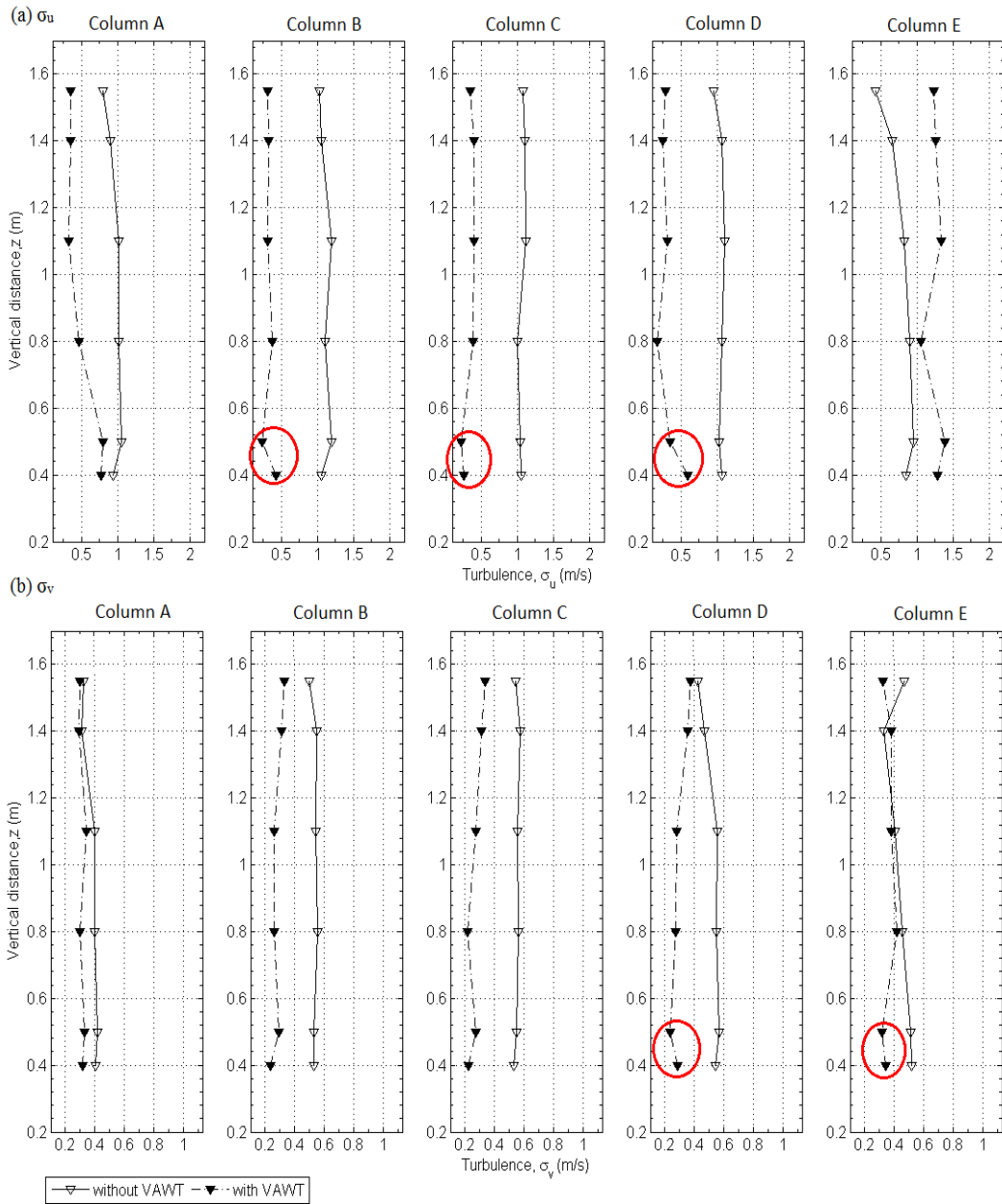


Figure 8. Vertical profile of longitudinal and lateral turbulence intensities (σ_u and σ_v) distribution from bottom to top for each column (A to E) for the entire windswept area at high speed at downwind position; inverted triangle symbol represents downwind position without VAWT while filled inverted triangle symbol represents downwind position with VAWT; the circle indicates the deflection of flow by the bottom surface, which increased the turbulence intensity.

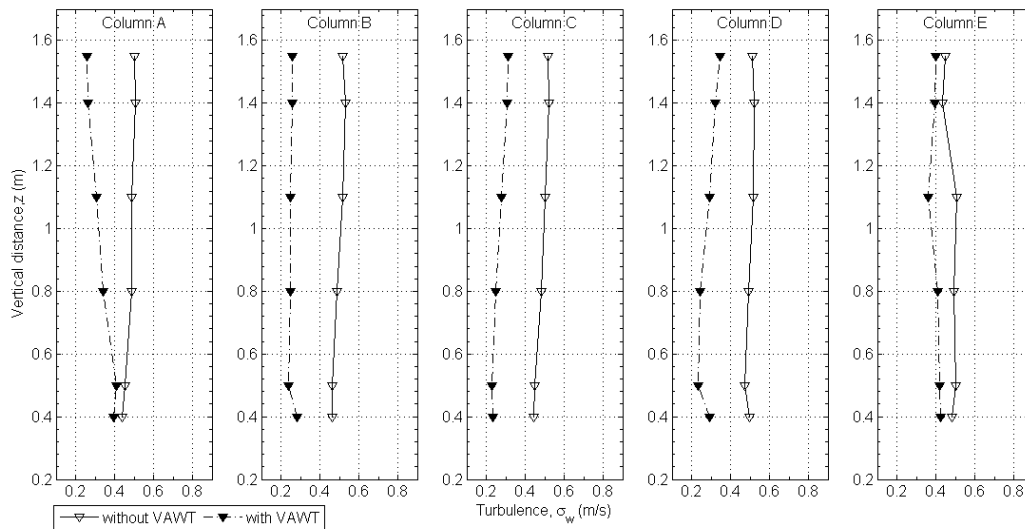


Figure 9. Vertical profile of vertical turbulence intensity (σ_w) distribution from bottom to top for each column (A to E) for the entire windswept area at high speed at downwind position; inverted triangle symbol represents downwind position without VAWT while filled inverted triangle symbol represents downwind position with VAWT.

CONCLUSIONS

The lateral and vertical profiles of turbulence of a VAWT were presented and discussed. The results presented are limited within certain flow velocities, ranging below 4.0 m s^{-1} . The turbulence and flow velocity distribution pattern were independent on the flow speed settings. Both low and high speeds exhibited the same turbulence distribution albeit at lower magnitudes. The rotational direction of VAWT (anti-clockwise) had led to the increment of σ_u from left to right. Meanwhile, the reverse flow generated by VAWT act as a resistance to the flow. The flow velocity was directed to the concurrent column of the VAWT. At downwind positions, VAWT dispersed the flow and thus the mean flow velocity subsequently decreased. The VAWT also reduced the turbulence, σ_u and σ_v . Turbulence transferring downwards caused vertical momentum transfer while some turbulences were added to the flow behind VAWT due to the deflection of the flow by the surface, which also increased turbulence. This study served as a comprehensive direct measurement of flow and turbulence using the eddy covariance method that could assist in developing techniques for quantifying turbulence of vertical axis wind turbines though limited to indoor conditions.

ACKNOWLEDGMENTS

The authors express their gratitude to the Malaysian Ministry of Education and Universiti Sains Malaysia (USM) by awarding the Fundamental Research Grant

Scheme (FRGS) (grant no.: 203/PTEKIND/6711329) and the USM short-term grant (grant no.: 304/PTEKIND/6312099) to conduct this research.

REFERENCES

1. Shafiullah, G.M., A.M.T. Oo, A.B.M.S. Ali, and P. Wolfs, 2013. Potential challenges of integrating large-scale wind energy into the power grid - A review. *Renewable & Sustainable Energy Reviews*, 20: 306-321.
2. Mertens, S., *Wind Energy in Urban Area*. 2002 Delft University of Technology: Holland.
3. Balduzzi, F., A. Bianchini, E.A. Carnevale, L. Ferrari, S. Magnani, 2012. Feasibility analysis of a Darrieus vertical-axis wind turbine installation in the rooftop of a building. *Applied Energy*, 97: 921-929.
4. Dayan, E., 2006. Wind energy in buildings: Power generation from wind in the urban environment - where it is needed most. *Refocus*, 7: 33-38.
5. H'ng, Y., Y. Yusup, H.P.S. Abdul Khalil, and T. Teng, 2014. Pilot study on indoor flows and turbulence statistics of a vertical axis wind turbine. *Mechanical Engineering Research*, 4: 63-78.
6. Dabiri, J.O., 2011. Potential order-of-magnitude enhancement of wind farm power density via counter-rotating vertical-axis wind turbine arrays. *Journal of Renewable and Sustainable Energy*, 3: 043104(1-12).
7. Kinzel, M., Q. Mulligan, and J.O. Dabiri, 2013. Energy exchange in an array of vertical axis wind turbines. *Journal of Turbulence*, 14: 38-39.
8. Cristobal, U.R.N., A. Gallegos-Munoz, and R.A.J. Manuel. Numerical Analysis of a Rooftop Vertical Axis Wind Turbine. in *ASME 2011 5th International Conference on Energy Sustainability*, Parts A, B, and C2012. Washington, DC, USA.
9. Ebert, P.R. and D.H. Wood, 1997. The near wake of a model horizontal-axis wind turbine - I. Experimental arrangements and initial results. *Renewable Energy*, 12: 225-243.

10. Fernando, M.S.U. and V.J. Modi, 1989. A numerical-analysis of the unsteady-flow past a Savonius wind turbine. *Journal of Wind Engineering and Industrial Aerodynamics*, 32: 303-327.
11. Vermeer, L.J., J.N. Sorensen, and A. Crespo, 2003. Wind turbine wake aerodynamics. *Progress in Aerospace Sciences*, 39: 467-510.
12. Yang, Z.F., P. Sankar, and H. Hu, 2012. Visualization of the tip vortices in a wind turbine wake. *Journal of Visualization*, 15: 39-44.
13. Yao, J., J.L. Wang, W.B. Yuan, H.M. Wang, L. Cao, 2012. Analysis on the influence of turbulence model changes to aerodynamic performance of vertical axis wind turbine. *International Conference on Advances in Computational Modeling and Simulation*, 31: 274-281.
14. Breton, S.P., K. Nilsson, S. Ivanell, H. Olivares-Espinosa, C. Masson, and L. Dufresne, 2012. Comparative CFD study of the effect of the presence of downstream turbines on upstream ones using a rotational speed control system. *Science of Making Torque from Wind* 2014. 555.
15. Barthelmie, R.J., L. Folkerts, G.C. Larsen, K. Rados, S. T. Frandsen, S. C. Pryor, B. Lange, and G. Schepers, 2006. Comparison of wake model simulations with offshore wind turbine wake profiles measured by sodar. *Journal of Atmospheric and Oceanic Technology*, 23: 888-901.
16. Tabrizi, A.B., J. Whale, T. Lyons, and T. Urmee, 2015. Rooftop wind monitoring campaigns for small wind turbine applications: Effect of sampling rate and averaging period. *Renewable Energy*, 77: 320-330.
17. Troldborg, N., J.N. Sorensen, and R. Mikkelsen, 2007. Actuator line simulation of wake of wind turbine operating in turbulent inflow - art. no. 012063. *Science of Making Torque from Wind*, 75: 12063-12063.
18. Hunt, J.C.R. and J.F. Morrison, 2000. Eddy structure in turbulent boundary layers. *European Journal of Mechanics B-Fluids*, 19: 673-694.

Persian Abstract

DOI: 10.5829/idosi.ijee.2016.07.02.01

چکیده

اندازه گیری های شدت تلاطم ناشی از محور عمودی توربین بادی (VAWT) برای تعیین کارایی و عملکرد ضروری است. در این بررسی، روش کوواریانس گرداب (EC) برای مشخصه یابی جریان استفاده شده است و مستقیماً تلاطم VAWT در یک آزمایشگاه سرپوشیده با استفاده از بادسنج اولتراسونیک (در ده هرتز) در موقعیت های مشخصی از دریچه توری هم در مسیر جریان باد و هم در خلاف مسیر باد (در دنباله) از VAWT اندازه گیری کردند. در تقابل با شبیه سازی های عددی، این روش پتانسیل آن را دارد که با دقت بالایی تلاطم توربین های بادی را بطور کمی بیان کند. بنابراین قادر به توصیف تجربی الگوهای جریان حول VAWT هستند. نتایج نشان داده اند که در موقعیت خلاف مسیر باد، بعضی از منطقه های پیچ دار VAWT جریان را بدلیل جریان های جاری همزمان که از چرخش محور چرخان تولید شده اند، مسدود کردند در حالی که باعث می شود بعضی از این جریان ها منحرف شده و به منطقه جریان همزمان VAWT اضافه شود. در دنباله VAWT، سرعت های جریان و تلاطم کاهش پیدا کردند و پراکنده شدند در حالی که در خط میانی، تلاطم میانی به طرف ته منطقه پیچ دار کاهش پیدا کرد. این انتقال سرازیری تلاطم بطور کلی باعث انتقال مومنت عمودی منفی شد. اگرچه، افزایش جزئی تلاطم در منطقه زمینه ای بدلیل انحراف جریان مشاهده شد.
